Research Article –submitted to Molecular Biology and Evolution Discoveries

# Compatibility of evolutionary responses to constituent antibiotics drive resistance evolution to drug pairs

**Authors:** Leonie Johanna Jahn, Daniel Simon, Mia Jensen, Charles Bradshaw, Mostafa Mostafa Hashim Ellabaan, Morten Otto Alexander Sommer

Novo Nordisk Foundation Center for Biosustainability, Technical University of Denmark, DK-2800 Kongens Lyngby, Denmark

Correspondence should be addressed to
M.O.A.S.: msom@bio.dtu.dk

**Abstract**

Antibiotic combinations are considered a relevant strategy to tackle the global antibiotic resistance crisis since they are believed to increase treatment efficacy and reduce resistance evolution (World Health Organization and Global Tuberculosis Programme, 2016). However, studies of the evolution of bacterial resistance to combination therapy have focused on a limited number of drugs and have provided contradictory results (Hegreness et al., 2008; Lipsitch and Levin, 1997; Munck et al., 2014). To address this gap in our understanding, we performed a large-scale laboratory evolution experiment, adapting 8 replicate lineages of *Escherichia coli* to a diverse set of 22 different antibiotics and 33 antibiotic pairs. We found that combination therapy significantly limits the evolution of *de novo* resistance in *E. coli,* yet different drug combinations vary substantially in their propensity to select for resistance. In contrast to current theories, the phenotypic features of drug pairs are weak predictors of resistance evolution. Instead, the resistance evolution is driven by the relationship between the evolutionary trajectories that lead to resistance to a drug combination and those that lead to resistance to the component drugs. Drug combinations requiring a novel genetic response from target bacteria compared to the individual component drugs significantly reduce resistance evolution. These data support combination therapy as a treatment option to decelerate resistance evolution and provide a novel framework for selecting optimized drug combinations based on bacterial evolutionary responses.

## Introduction

The prevalence of antibiotic resistance has become a global health concern, limiting the efficacy of standard treatments for acute and chronic bacterial infections (Ventola, 2015). As the development of novel antibiotics is expensive in terms of time and resources (Luepke et al., 2017), it is important to use currently available drugs in the best possible way to decelerate antibiotic resistance evolution and to maximize positive treatment outcomes. Empiric combination therapy is believed to improve treatment outcomes via increased potency and reduced evolution of drug resistance( Bantar et al., 2004; Blomberg et al., 2001). However, the clinical benefit of combination therapy remains controversial (Bantar et al., 2004; Bliziotis et al., 2005; Leibovici et al., 1997; Lipscey et al., 2018; Paul, 2014; Skorup et al., 2014; Tepekule et al., 2017). The disparate results might be explained by an incomplete understanding of the factors that drive the evolution of resistance to combination therapy.

Drug combinations have been mainly studied in regards to phenotypic characteristics such as drug interaction (Barbosa et al., 2018; Baym et al., 2016; Hegreness et al., 2008; Munck et al., 2014; Torella et al., 2010) or collateral drug responses (de Evgrafov et al., 2015; Munck et al., 2014). Drug interactions describe the combined effect of multiple drugs relative to the sum of their individual effects (additive, synergistic and antagonistic)(Wong, 2017). Collateral drug responses occur when a bacterium that evolved resistance to a drug displays higher susceptibility (collateral sensitivity) or increased resistance (collateral resistance) to other agents (Beutner et al., 1963; Szybalski and Bryson, 1952). These different phenotypic characteristics have been correlated with resistance evolution in multiple studies with contradictory results ranging from accelerated to decelerated evolution (Barbosa et al., 2018; Hegreness et al., 2008; Munck et al., 2014).

In addition, the genetics underlying the resistance evolution towards drug combinations have only been studied for a very limited number of drug pairs (de Evgrafov et al., 2015; Munck et al., 2014; Suzuki et al., 2015). Two small-scale studies identified that mutations linked to collateral sensitivity were less prominent in the combination of collateral sensitive drugs (Munck et al., 2014; Suzuki et al., 2015), while another study found that the types of mutations are different in drug pair evolved lineages compared to single drug evolved ones (Laehnemann et al., 2014). Yet, the genetic trajectories towards drug combinations have not been characterized systematically under controlled conditions along with their potential to predict resistance evolution.

In order to address this lack of knowledge we conducted a systematic high-throughput adaptive laboratory evolution experiment for *Escherichia coli,* an important model organism and human pathogen (Bodilsen et al., 2018). The large number of replicate lineages and the broad range of drugs tested combined with a systematic assessment of the evolvability allowed us to analyze the phenotypic and genotypic evolutionary responses to single and combinatorial drug exposure. Based on this comprehensive dataset we identified for the first time distinct patterns in the genetic responses towards drug combinations. Moreover, these genetic trajectories are reliable predictors for the evolvability of antibiotic resistance.

## Results

Resistance evolution towards a diverse set of antibiotic combinations

To identify the underlying features that drive the evolution of resistance to combination therapy, we adapted genetically barcoded replicate lineages (Jahn et al., 2018) of the well-studied model organism *Escherichia coli* K12 MG1655 to a diverse set of 22 different antibiotics and 33 different antibiotic pairs (Table S1, Table S2). These drugs, including both bactericidal (68.18%) and bacteriostatic (31.81%) drugs, covered 11 different drug classes and targeted 6 different bacterial processes (Table S2, Fig. 1a). Moreover, we assessed the phenotypic features of the drug pairs. First, we classified the drug combinations based on the drug interaction and found that they covered all three possible drug interactions: synergistic (34.4%), additive (28.1%) and antagonistic (37.5%) (Fig. 1b). The classification was done by measuring the drug concentration that resulted in a 90% growth-reduction ($IC_{90}$) of the wild type (WT) compared to WT growth in media only for all single antibiotics and for the antibiotics in combination. Based on these values the fractional inhibitory concentration index was calculated (FICI) (Tyers and Wright, 2019). While different methods to calculate drug interactions are used that impact the classification of drug interactions, we decided to use a Loewe-additivity model based on the $IC_{90}$ (which is similar to the minimal inhibitory concentration (MIC)) as this is commonly reported in scientific studies and allows best possible comparison of our study with the existing literature (Gonzales et al., 2015; Minato et al., 2018; Munck et al., 2014; Stokes et al., 2017; Tyers and Wright, 2019). Further, we defined cut-offs for the FICI (Materials and Methods) to distinguish between the drug interactions: antagonistic (ANT, FICI > 1.5), additive (ADD, FICI = 0.75-1.5) and synergistic (SYN, FICI < 0.75),

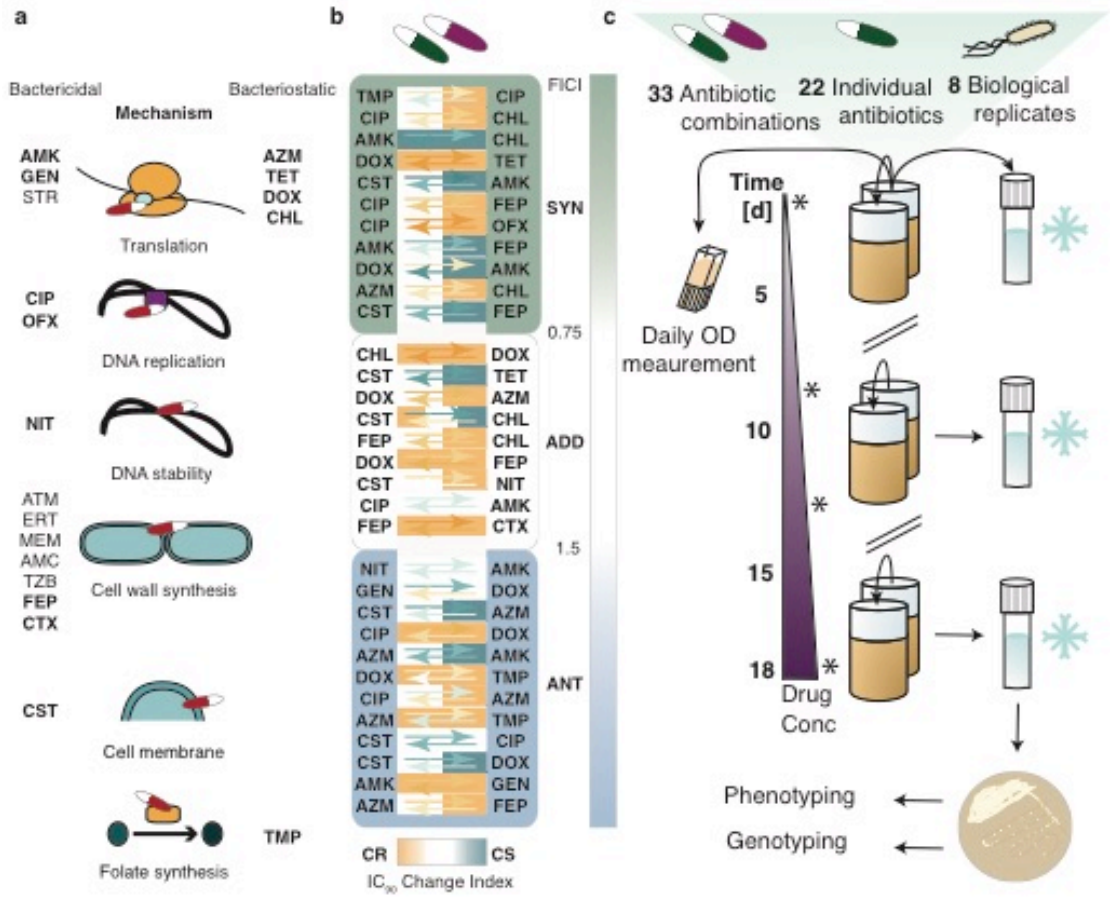


**Figure 1:** Drug properties and experimental setup. **a** Characteristics of the drugs chosen for adaptive laboratory evolution. The antibiotics were either bactericidal or bacteriostatic and covered multiple drug classes and six different processes in the cell. Drugs chosen for the evolution in drug pairs are depicted in bold. **B** The drug pairs, shown in ascending order of the fractional inhibitory concentration index (FICI), exhibit various phenotypic interactions: synergy (SYN, FICI < 0.75, green), additivity (ADD, FICI = 0.75-1.5, white) and antagonism (ANT, FICI > 1.5, blue); collateral resistance (CR, orange), a neutral collateral response (N, white) and collateral sensitivity (CS, turquoise). The arrows show the fold increase (orange, CR > 2 * median ancestral wild type (WT) $IC_{90}$) or decrease (turquoise, CS < 0.5 * median WT $IC_{90}$) in resistance compared to the WT. The direction of the arrows indicates the direction of the collateral drug response: e.g. lineages evolved to Trimethoprim display mild collateral resistance to Ciprofloxacin, while lineages evolved to Ciprofloxacin show mild collateral sensitivity to Trimethoprim. The space around the arrows is colored based on the classification of the drug pairs as CR, CS or neutral according to the collateral $IC_{90}$ change index of each isolated biological replicate. Definitions of antibiotic abbreviations can be found in Table

S2. Definitions of the different categories (SYN, ADD, ANT, CS, CR) as well as definitions of the FICI, $IC_{90}$ and collateral $IC_{90}$ change index can be found in materials and methods. The figure lists 32 antibiotic pairs due to the exclusion of the replicate lineages evolved to Sulfamethoxazole-Trimethoprim, as Sulfamethoxazole appeared unstable upon freezing, resulting in unreliable resistance determination. **c** Adaptive laboratory evolution of antibiotic resistance. Genetically barcoded *E. coli* lineages were evolved in eight biological replicate lineages with 22 different antibiotics and 33 different antibiotic combinations. The replicate lineages were grown in 96-deep-well-plates in 1 ml of LB containing antibiotic. Every 22 h, the cells were transferred to a new plate in a 20-fold dilution. In addition, the optical density was measured immediately before each transfer, and an aliquot of the population was saved as a glycerol stock. The evolution of resistance in each replicate lineage was monitored by measuring the $IC_{90}$ at day 0, 8, 13 and 18, as indicated with stars. The evolution was started at subinhibitory drug concentrations (25 % of the WT $IC_{90}$), and the WT $IC_{90}$ was reached on the 7$^{th}$ day of the experiment. The evolution experiment ended after 18 days, when the WT $IC_{90}$ was exceeded by more than 10-fold. Isolated colonies were obtained from frozen endpoints and subsequently used for whole-genome sequencing and susceptibility testing to multiple antibiotics.

Resistance to these drugs and drug combinations was achieved via adaptive laboratory evolution (Jahn et al., 2017). Even though adaptive evolution experiments simplify the growth conditions in human hosts, they can capture clinically relevant features of resistance evolution (Imamovic et al., 2018). In addition, adaptive evolution reduces the complexity of resistance evolution in clinical settings and allows studying specific parameters systematically under controlled conditions (Jansen et al., 2013). We performed the evolution experiment in a stepwise manner (Jahn et al., 2017), in eight biological replicate lineages giving a total of 460 lineages (including 20 LB-only controls) (Fig. 1c, methods, antibiotic concentrations in Table S3). A single isolated colony was obtained for each revived endpoint lineage for subsequent genotypic and phenotypic characterizations (Table S4). After the adaptive evolution experiment, we measured the $IC_{90}$ of all isolates. In order to check whether the isolates were representative for the lineage they were obtained from, we calculated the difference between the $IC_{90}$ of the lineages and the $IC_{90}$ of the isolates derived from the respective lineages and normalized it by the lineage $IC_{90}$, similar to the calculation of the Coefficient of variance. The median of these indices was 0.66 indicating an acceptable agreement between isolates and lineage $IC_{90}$s. However, certain antibiotics like beta-lactams and

many drug combinations had higher or lower lineage resistance compared to the isolates (Fig. S1). This might be the result of different aspects such as population dynamics (Lee et al., 2010), inoculum effect (Brook, 1989), tolerance (Levin-Reisman et al., 2017) and selection bias of the isolates due to freezing sensitivity (Barbosa et al.).

We also measured the $IC_{90}$ of all isolates adapted to single-drugs towards all single drugs used. The resulting data allowed us to assess collateral drug responses (Fig. S2). Therefore, the drug pairs could be grouped based on the collateral $IC_{90}$ change index into one of three categories: collateral resistant (CR, collateral $IC_{90}$ change index > 2), collateral sensitive (CS, collateral $IC_{90}$ change index < 0.5) or neutral (N, collateral $IC_{90}$ change index 0.5-2). The collateral $IC_{90}$ change index provides the average change in fold resistance relative to the WT between two isolates adapted to either drug A or B to the respective other drug (Munck et al., 2014). We found that the drug pairs displayed all possible collateral responses between the individual drugs constituting the pairs (Fig. 1b).

Assessment of evolutionary responses to combination therapy

Before we analyzed the isolates, we also observed the behavior of the entire populations during the adaptive evolution experiment. A majority (68.4%) of the lineages adapted to monodrug exposure exhibited stable growth throughout the evolution experiments (chi-square test of independence, $X^2$ = 84.742, $p$ = 2.2e-16, df = 1, n(Mono) = 152, n(Combination) = 256). In contrast, most (59.4%) of the lineages exposed to drug combinations exhibited declining OD values over time (chi-square test of independence, $X^2$ = 37.028, $p$ = 1.164e-09, df = 1, n(Mono) = 152, n(Combination) = 256) (Fig. S3a-c). Declining OD values might indicate that the populations did not evolve resistance at a sufficient pace to ensure survival. Further, we measured the resistance level of the lineages at different time points during the experiment. We calculated the Coefficient of variance (CV) of the endpoint $IC_{90}$ levels of the parallel-evolved lineages and found a significant (Mann-Whitney U-test, $p$ = 0.003076, U = 2552, two-sided, confidence level = 0.95) difference between the variance of single-drug (CV = 0.388417) and drug pair (CV = 0.6410415) evolved lineages. Usually, a higher degree of phenotypic convergent evolution is associated with a higher selection pressure and constrained evolution (MacPherson and Nuismer, 2017), yet parallel evolution is also highly depended on population size (Bailey et al., 2015). As mentioned before drug pair evolved lineages had often decreasing population sizes, which might account for the higher phenotypic variability.

Looking at the $IC_{90}$ data of the lineages during the evolution experiment, we found that after completion of the evolution a majority (67.8%) of the drug-pair-evolved replicate lineages, but a minority (23.5%) of the single-drug-evolved lineages, only gained resistance levels below the antibiotic concentration they were exposed to during the adaptive laboratory evolution (chi-square test of independence, $X^2$ = 73.117, $p$ = 2.2e-16, df = 1, n(Mono) = 152, n(Combination) = 256) (Fig. S3d-f). This observation suggests a limited capacity of drug-pair-exposed lineages to evolve resistance.

Combination therapy reduces resistance evolution

To further examine resistance evolution we assessed the phenotypes of the isolated colonies from the end point of the evolution experiment. We found that isolates evolved to about half of the drug pairs (15) displayed resistance to the drug pair and the individual drugs constituting the pair. For the other drug combinations we observed resistance to the drug pair and only one of the individual drugs (eight drug pairs), only to one of the individual drugs (five drug pairs) or no resistance at all (four drug pairs). This observation highlights variable abilities to evolve resistance and different dynamics of the drug pairs to select for adaptations.

To shed light on the factors that impact resistance evolution, we calculated the evolvability index for all drug pair-evolved lineages (Munck et al., 2014). The evolvability index describes the final phenotypic adaptation level relative to single-drug-evolved isolates (Munck et al., 2014). All the isolates except those evolved to a combination of ciprofloxacin and azithromycin had a median evolvability index less than 1, indicating that the drug-pair-evolved isolates became less resistant to the two individual drugs than the isolates evolved to these drugs alone (Fig. 2). In fact, for a majority of the drug pairs (87.5%), very limited resistance evolution was observed (evolvability index < 0.5).

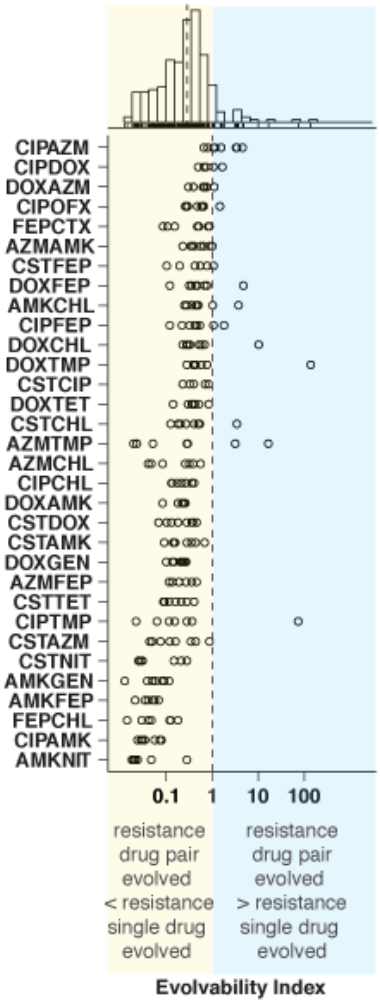


**Figure 2:** Antibiotic combinations limit resistance evolution. Distribution of the evolvability index of the different isolates from replicate lineages each represented with a dot for each drug pair. Drug pairs are ordered by median evolvability index. The histogram displays a unimodal right skewed distribution of the isolates over the evolvability index. The dotted line in the histogram indicates the median. Explanations for outliers are discussed in Table S5.

These findings highlight that drug pairs in general reduce the adaptive potential of *de novo* antibiotic resistance evolution in *E. coli*. Nevertheless, *E. coli* evolved resistance to specific drug combinations to a markedly different degree.

Phenotypic features impact evolvability only marginally

Prior studies have suggested that drug features like synergistic or antagonistic drug interactions or collateral drug responses play an important role in explaining the difference in resistance evolution toward drug combinations (Barbosa et al., 2018; Hegreness et al., 2008; Munck et al., 2014; Suzuki et al., 2015) (Fig. 3a). We grouped the

drug pairs into antagonistic, additive and synergistic based on the FICI. However, we observed only a minor contribution of synergistic or antagonistic drug interactions on the evolvability of resistance (Fig. 3b). Further, we did not find a correlation between the FICI and the evolvability index (Fig. 3c). Next, we assessed the effect of collateral responses on evolution of resistance to drug combinations by grouping the drug pairs based on the collateral $IC_{90}$ change index. Again, we observed only a limited effect of collateral responses on the evolvability index (Fig. 3d) and no significant correlation between the collateral $IC_{90}$ change index and the evolvability index (Fig. 3e).

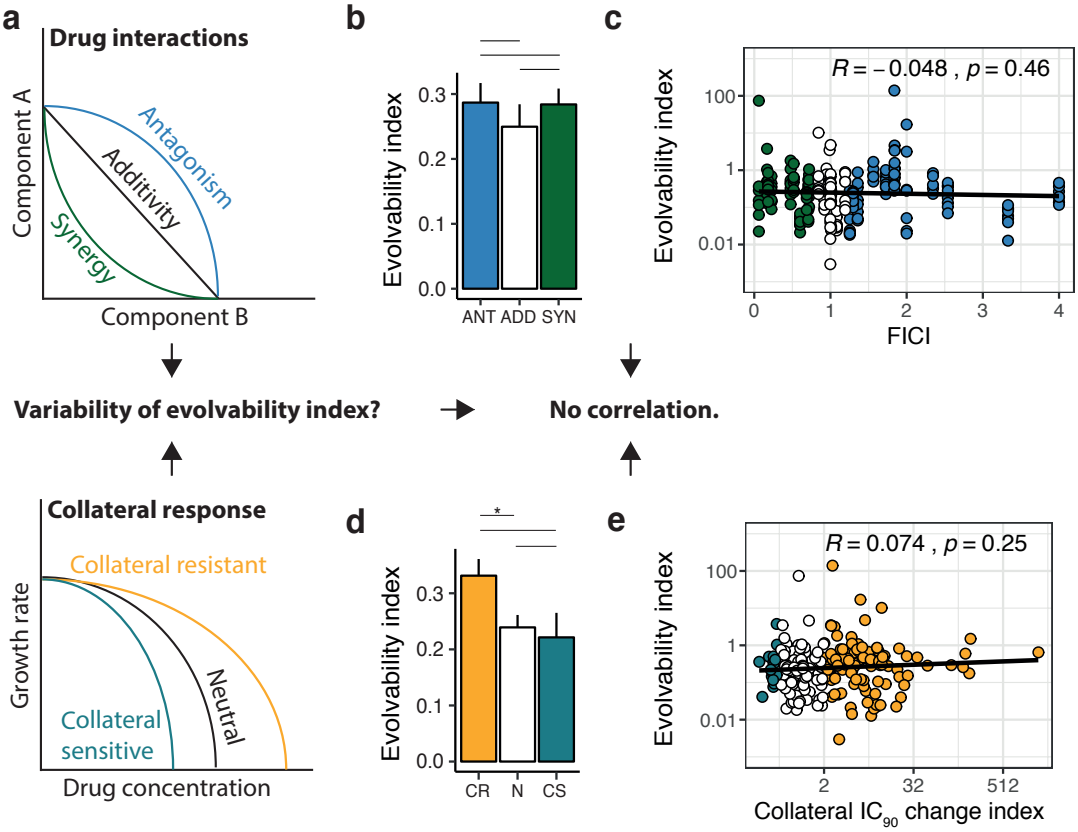


**Figure 3:** Phenotypic features of drug combinations are weak predictors of the evolvability. ANT = antagonistic drug pairs; ADD = additive drug pairs; SYN = synergistic drug pairs. CR = collateral resistance; N = neutral; CS = collateral sensitivity. **a** Schematic overview of the different types of drug interaction and collateral drug responses. It has been hypnotized previously that they might impact the evolvability of drug combinations. **b**The median evolvability indices (±MAD) for drug pairs grouped by the FICI (Mann-Whitney U-test, median(ANT) = 0.29, n(ANT) = 83, median(ADD) = 0.23, n(ADD) = 71, median(SYN) = 0.28, n(SYN) = 83, ANT-ADD: $p$ = 0.3251, U = 3218.5, ANT-SYN: $p$ = 0.8806, U = 3491.5, ADD-SYN: $p$ = 0.3873, U = 3185.5, Bonferroni corrected,

two-sided, confidence level = 0.95). **c** Scatterplot of the evolvability index versus FICI (Pearson correlation coefficient R = -0.048, $p$ = 0.46). **d** Median evolvability indices (±MAD) for drug pairs grouped by the collateral $IC_{90}$ change index (Mann-Whitney U-test, median(CR) = 0.36, n(CR) = 108, median(N) = 0.23, n(N) = 110, median(CS) = 0.22, n(CS) = 19, CR-N: $p$ = 0.01654, U = 7056.5, CR-CS: $p$ = 0.245, U = 1198.5, N-CS: $p$ = 0.7397, U = 1095.5, Bonferroni corrected, two-sided, confidence level = 0.95). **e** Scatterplot of the evolvability index versus the collateral $IC_{90}$ change index (Pearson correlation coefficient R = 0.074, $p$ = 0.25).

Genetic responses to drug pairs follow distinct patterns

To determine the genetic basis of resistance and to assess if the genotypes could explain the varying levels of evolvability among the different drug pairs, we performed whole-genome sequencing on 313 of the phenotypically characterized isolates that exhibited phenotypic resistance ($IC_{90}$ > 2-fold WT $IC_{90}$) after an initial screening (Table S6). In total, we found 1062 single nucleotide variants, 1052 gene duplications and 368 insertions or deletions (Table S7). Six isolates displayed a hypermutator phenotype with between 21 and 383 mutations. All hypermutators had a mutation in either *mutS, mutT* or *mutD* (*dnaQ*) (Table S7), which induce the hypermutator phenotype (Jolivet-Gougeon et al., 2011). On average, we detected approximately 5 mutations per isolate. The number of mutations per isolate was roughly the same between isolates adapted to a single or to multiple antibiotics (Fig. S4). However, the types of mutations differed. While single nucleotide polymorphisms (SNP) were the dominant response under single drug exposure, gene duplications were most prevalent in drug pair evolved isolates, as reported before (Laehnemann et al., 2014). The gene that was mutated the most (101 times + 15 times in the promoter region) was *marR* (Table S7), the regulator of the multiple antibiotic resistance locus (Cohen et al. 1993), a gene in which mutations can induce a multidrug resistance phenotype (Woodford and Ellington, 2007). Antibiotic resistance is facilitated through MarR by the transcriptional regulation of at least 80 chromosomal genes (Pomposiello et al. 2001, Barbosa et al. 2000, Alekshun et al. 1997), involving primarily stress response (Alekshun et al. 1997) and multidrug efflux (Keeney et al. 2008). Multiple other mutations are also known to be linked to a multidrug resistance phenotype and often involve acrB-mediated efflux of the antibiotic (Okusu et al., 1996) and have been identified in this study (Table S7). The multidrug resistance induced through these mutations can be illustrated by clustering the antibiotic evolved isolates based on their genetic similarity. We calculated the genetic similarity of all single drug evolved isolates based on the Jaccard's Distance and found that isolates

evolved to different drugs like tetracyclines, chloramphenicol, beta-lactam and macrolide antibiotics clustered together (Fig. S5). This finding highlights that resistance mechanisms evolve that are not necessarily specific to the mechanism of action of the antibiotic. In addition, the genetic similarity can also explain collateral resistance as genetic similarity and collateral resistance are positively correlated (Fig. S6).

We grouped drug-pair-evolved isolates into four distinct genetic responses relative to their genetic response towards their constituent drugs : (1) mutations conferring resistance to both constituent drugs are the same and are selected by the drug combination (Shared genotype); (2) mutations conferring resistance to both constituent drugs are different, yet are both selected by the drug combination (Mixed genotype); (3) mutations conferring resistance to both constituent drugs are different, yet only mutations for one of the constituent drugs are selected by the drug combination (One Drug genotype); or (4) mutations selected by the drug combination are different from those selected by each of the constituent drugs (New genotype) (Fig. 4a). To classify the drug pairs into these distinct categories, we performed an analysis of similarities (ANOSIM) based on the mutations of each sequenced isolate (Table S7). ANOSIM is a nonparametric statistical test that is widely used in ecology to identify differences among ecological niches based on ranked dissimilarity matrices (Bueno et al., 2018). Here, we used mutated genes as features to identify differences between various adaptation conditions instead of characteristics of an ecological niche.

The Shared group contained three drug pairs for which no significant genotypic differences ($R < 0.2$ and/or $p > 0.005$, Table S8) were observed between single-drug-evolved isolates or between single-drug-evolved isolates and drug-pair-evolved isolates (Fig. 4b). For example, key mutations found in doxycycline-adapted isolates were also dominant in chloramphenicol-evolved isolates as well as isolates exposed to both drugs simultaneously. All drug pairs belonging to the Shared group exhibited collateral resistance to each other (Fig. S7), as the genetic alterations provide resistance to both individual drugs as well as to the drug pair.

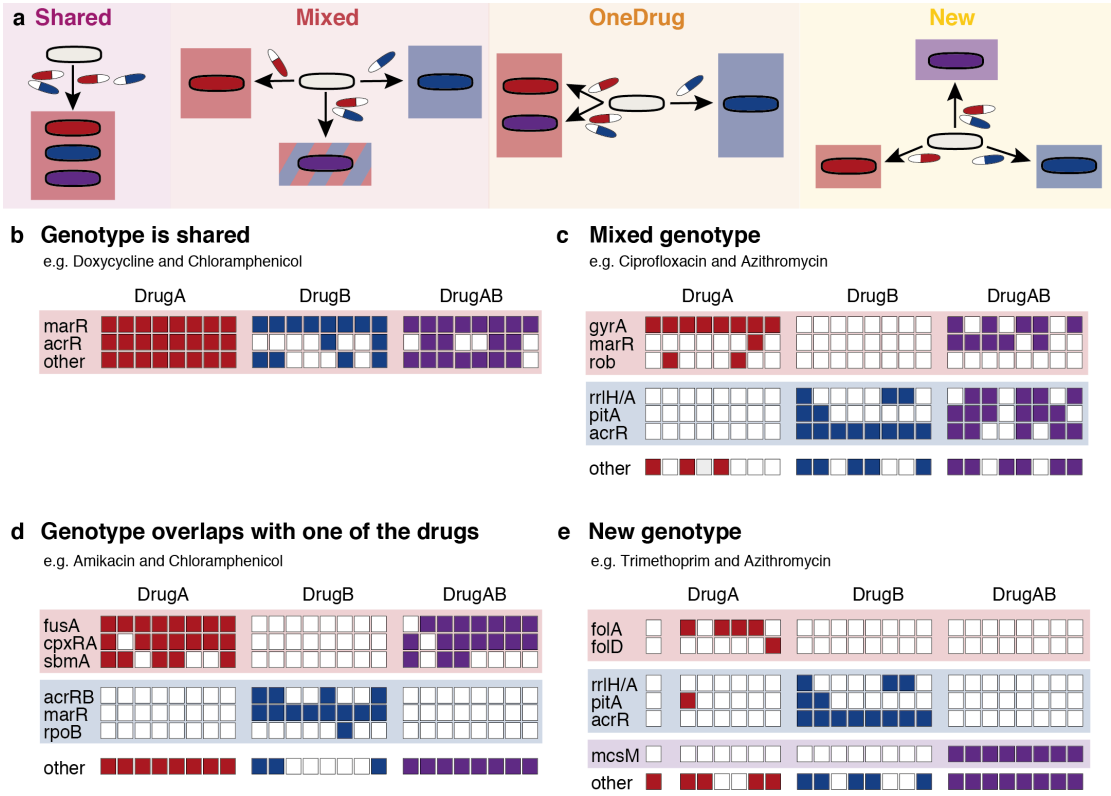


**Figure 4:** Drug pairs can be grouped in four distinct categories based on their genotypic response in relation to the genotype of isolates adapted to the constituent drugs. **a** Schematic overview of the possible genetic responses of drug-pair-evolved isolates compared to those evolved to the component drugs. **b – e** Examples of the genotypes of the eight replicates of single-drug-evolved and drug-pair-evolved isolates for each genetic group.

The Mixed group contained two drug pairs, where a significant difference ($R > 0.2$ and $p < 0.005$, Table S8) between the genotypes of isolates evolved to individual drugs was observed, but no significant difference was observed between the genotypes of drug-pair-evolved isolates and those of isolates evolved to individual drugs (Fig. 4c). For example, while the genotypes of isolates evolved to either ciprofloxacin or azithromycin were completely different, the drug-pair-evolved isolates exhibited key mutations that were also found in the isolates exposed to the individual drugs (Fig. 4c). This drug combination was also the only one that had a median evolvability index greater than 1, indicating that compatible genetic pathways are unlikely to reduce the evolvability. The two drug pairs with a Mixed genotype exhibited either neutral or collateral resistance to each other, further highlighting that these drug pairs have compatible genetic responses (Fig. S7).

The One Drug group was composed of drug pairs where the genotype exclusively resembled that of isolates evolved to one of the individual drugs and contained 14 drug pairs (Fig. 4d). For example, mutations selected against amikacin were also present in the isolates exposed to amikacin and chloramphenicol, while none of the mutations found in chloramphenicol-adapted isolates were selected in the drug-pair-evolved isolates. Five drug pairs in the One Drug group reached only final exposure levels around the $IC_{90}$ of the individual drugs, mainly due to synergism (Fig. S7). This finding indicates that adaptation to highly synergistic drug pairs might be achieved by selection of mutations against one of the constituent drugs thereby possibly shifting the drug interaction profile. This would suggest that synergistic drug combinations could readily loose efficiency if used at insufficient doses, as previously suggested (Lipsitch and Levin, 1997; Pena-Miller et al., 2013). Other factors influencing the selection of mutations towards one of the drugs might be differences in the steepness of the dose response curves (Chevereau and Bollenbach, 2015) and accordingly different levels of selection pressure applied by the two drugs (Fig. S8) as well as differences in the mutation selection window and the ability to select for mutations at subinhibitory concentrations (Fig. S9).

Another five of the drug combinations in the OneDrug group were resistant to both individual drugs and drug pairs. Drugs in these pairs were substrates of the AcrB efflux pump (Yu et al., 2003). While isolates adapted to one of the constituent drugs alone, such as ciprofloxacin, develop resistance primarily via other resistance modes, such as mutations in *gyrA*, isolates adapted to the other drug, such as doxycycline, select for efflux-enhancing mutations. In combination, the efflux mutations are dominant, as these mutations confer resistance to both drugs simultaneously and are therefore likely to be selected. Consequently, the resulting genotype resembles the genotype of the efflux-mutation-selecting single-drug-evolved isolates, even though a shared resistance mechanism is selected. Of the remaining drug combinations in the OneDrug group, two displayed collateral sensitivity, which might have suppressed resistance evolution to one of the drugs.

The New group included drug pairs for which the ANOSIM gave significant ($R > 0.2$, $p < 0.005$, Table S8) differences in genotypes between individual drugs and drug pairs (Fig. 4e). For example, azithromycin- and trimethoprim-adapted isolates shared almost no mutations, while the isolates evolved to the combination of azithromycin and trimethoprim selected none of these mutations but repeatedly accumulated mutations

in the mechanosensitive channel encoding gene *mscM.* Drug pairs with collateral sensitivity were found only in the OneDrug and New groups (Fig. S7), highlighting those incompatible genetic trajectories to the individual drugs cannot be co-selected in drug combinations.

Drug pairs requiring novel genetic responses exhibit the lowest evolvability index

To assess the impact of genotypic response on phenotypic evolvability, we analyzed the evolvability of the four different genetic groups. Drug pairs in the New group generally showed a lower evolvability index and a lower evolutionary rate (Fig. 5a). Of the five drug pairs that composed the New genotype group, three exhibited collateral sensitivity to each other in at least one direction and two were defined collateral sensitive based on the collateral $IC_{90}$ change index. All three contained an aminoglycoside antibiotic (Fig. S7). These drug pairs also had the lowest evolvability indices within the group. However, isolates evolved to azithromycin and trimethoprim also developed a distinct new genotype, despite a lack of collateral sensitivity.

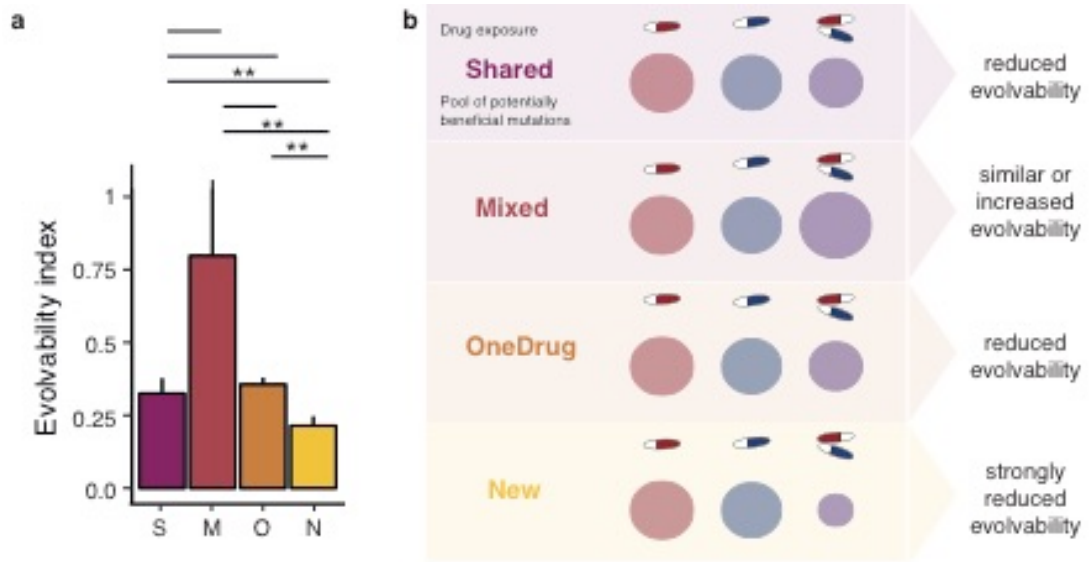


**Figure 5:** Drug pairs requiring a novel genetic response compared to the constituent drugs have a significantly lower resistance evolvability. S = Shared genotype; M = Mixed genotype; O = OneDrug genotype; N = New genotype. **a** The median evolvability index (±MAD) of drug combinations grouped by genetic response patterns (Mann-Whitney U-test, median(Shared) = 0.32, n(Shared) = 24, median(Mixed) = 0.8, n(Mixed) = 15, median(OneDrug) = 0.36, n(OneDrug) = 99, median(New) = 0.21, n(New) = 39, Shared-Mixed: $p$ = 0.1308, U = 233, Shared-OneDrug: $p$ = 0.5815, U = 1146, Shared-New: $p$ = 0.008947, U = 291, Mixed-OneDrug: $p$ = 0.0697, U = 997.5, Mixed-New: $p$ = 0.009358, U

= 438, OneDrug-New: $p$ = 0.002111, U = 1376, Bonferroni corrected, two-sided, confidence level = 0.95). **b** Schematic overview of the different drug regimes (single drug A, single drug B and drug pair A and B) and the pool of potentially beneficial mutations that can confer resistance. We hypnotize that the adaptation potential of the Shared and OneDrug groups are comparable to the ones of the individual drugs, maybe slightly smaller due to few genetic constrains. The pool of beneficial mutations of the mixed group might in fact be bigger than the two pools of the single drugs as mutations against both drugs can be selected for. This might explain why the evolvability of drug pair evolved isolates in the mixed group can be higher than the evolvability of single drug evolved isolates. The New group has a much smaller pool of beneficial mutations, as the adaptations against the individual drugs are not compatible, reducing the options for adaptations and therefore the evolvability.

Overall, these findings highlight that drug combinations work best at decelerating resistance evolution when the resistance modes to the individual drugs are incompatible and require a novel genetic response (Fig. 5b). There appears to be a low probability of selection of these novel responses, as evolvability in this genetic group was significantly lower than that in the other groups (Fig. 5). Interestingly, collateral sensitivity might be an indicator for the genetic incompatibility as drug pairs with collateral sensitivity grouped exclusively in the New and OneDrug group (Pearson's Chi-squared test, $X^2$ = 16.381, $p$ = 0.01185, df = 6). By contrast, drug pairs that evolved resistance by selecting for mutations against both drugs, belonging either to the Mixed or Shared group and in part to the OneDrug groups, had higher evolvability indices (Fig. 5a), demonstrating that combinations of antibiotics that have compatible genetic responses are not well suited to limit resistance evolution.

## Discussion

This study aimed to assess the potential of antibiotic combinations in reducing resistance evolution and to identify key properties of these combinations that can predict resistance evolution. We observed that *de novo* antibiotic resistance evolution is reduced in *E. coli* when two antibiotics are combined. We further assessed the ability of phenotypic parameters such as drug interactions and collateral responses to predict the evolvability.

Previous studies reported conflicting abilities of synergistic or antagonistic drug interactions in limiting resistance evolution (Barbosa et al., 2018; Hegreness et al., 2008; Lipsitch and Levin, 1997; Munck et al., 2014; Pena-Miller et al., 2013; Torella et al., 2010). In line with Munck et al. (2014), we find that drug interactions are weak predictors for resistance evolution. In addition to drug interactions we also analyzed the impact of collateral drug responses on the evolvability of resistance to drug combinations. Previous work had shown a correlation between collateral sensitivity and limited resistance evolution. However, even though drug pairs with collateral sensitivity had a lower evolvability index as neutral or collateral resistant drug pairs, the difference was not significant. This could be due to the small sample size of collateral sensitive drug pairs or the experimental design that selected for a specific resistance level.

Yet, by systematically analyzing the genetic adaptations, we observed a clear pattern relating the genetic trajectories to resistance evolution. Grouping of drug pairs based on genotypes revealed that resistance evolution to drug pairs that required a new genotypic response relative to the genetic adaptations to the constituent drugs, was greatly limited. Future work in identifying further evolutionary constrained drug pairs and a framework to predict limited resistance evolution will be needed in order to identify the best drug combinations for limited resistance evolution.

In general, our data provides a comprehensive resource for the exploration of *de novo* resistance evolution in *E. coli* and of the different phenotypic and genotypic adaptations to monotherapy and combination therapy. However, the number of isolated colonies for each evolved lineage could be expanded in order to ensure that population heterogeneity and heteroresistance is captured sufficiently in the analysis and additional drug combinations and organisms would need to be characterized to elucidate whether our findings can be further generalized. In addition, the impact of drug combinations on the evolution of antibiotic tolerance should be addressed in future

work. Moreover, it remains to be determined whether our findings can be translated to the clinic. Adaptive evolution is frequently used to explore the response to antibiotic exposure (Imamovic and Sommer, 2013; Jahn et al., 2017; Lazar et al., 2014; Munck et al., 2014). However, factors, such as horizontal gene transfer, host-pathogen interactions, interactions between bacterial populations, side effects and pharmacodynamics of the antibiotics, as well as patient condition and disease, need to be considered when clinical experiments are conducted. Nonetheless, we expect that this framework for assessment of evolvability of drug combinations will be the base for further research on the rational design of drug combinations for efficient and resistance-limiting therapies.

## Materials and Methods

Bacterial strains and growth conditions

Chromosomally barcoded *Escherichia coli* MG1655 K12(Jahn et al., 2018) were grown in LB at 37 °C and 600 r.p.m. shaking. They were grown under the same conditions without shaking for the $IC_{90}$ determination.

Adaptive laboratory evolution (ALE) to individual drugs and drug combinations

*E. coli* lineages were evolved each in 8 biological replicate lineages to 22 different antibiotics and 33 different antibiotic pairs (Table S1) resulting in 460 individual lineages of which all *E. coli* lineages carried a unique genetic barcode (Jahn et al., 2018). Barcodes allowed to track lineages and to ensure that no cross-contamination between replicates took place. Moreover, genetically adapted lineages with barcodes can be provided as a valuable resource for additional experiments. All antibiotics used in this study, their mechanism of action, solvent and storage conditions are listed in Table S2. For the evolution towards drug combinations, the drugs were combined in a 1:1 ratio based on the WT $IC_{90}$ values of the individual drugs (Munck et al., 2014). The WT was exposed to a dilution series of the drug mixture, the $IC_{90}$ of the drug combination was established and used as a reference to define the antibiotic concentrations used for the adaptive evolution experiment (Table S3). The antibiotic pairs were chosen to cover the most important drug classes (beta-lactams, flourquinolones, aminoglycosides, macrolides, tetracyclines, chloramphenicol and peptide antibiotics) in all their possible combinations, to include drug pairs of drugs from the same drug classes and some additional drug pairs so that we could cover all possible drug interactions and collateral relation ships between drug pairs.

The adaptive evolution experiment was carried out in 96-deep-well plates. The plates were filled with LB by a Hamilton robot, sealed and stored at room temperature. Antibiotics were added by the robot the day before the experiment started and plates were stored at -20°C. An overnight culture grown in LB was used to inoculate the ALE experiments. All passaging of cells was done manually with an 8-channel pipette. As a control 20 replicates were evolved to LB media alone. Each 96-well plate also harbored 8 negative controls that stayed uncontaminated throughout the evolution experiment. Cells were grown for 22 h at 37 °C and 600 r.p.m. shaking, ensuring mixing of the population and aerobic growth conditions (aerobic growth conditions during the evolution can be assumed as genetic adaptations to aminoglycoside antibiotics, whose uptake depends on aerobic respiration, were identified as well as a mutational overlap

with other studies that had a greater surface:volume ratio (Munck et al., 2014) or better mixing (Hegreness et al., 2008)). Thereafter, 100 µl were transferred to a 96-well plate and the optical density ($OD_{600}$) of each lineage was measured in an ELx808 Absorbance Reader (BioTek) at a wavelength of 600 nm. In addition, 50 µl of cells, corresponding to a 20-fold dilution (Jahn et al., 2017; Wahl et al., 2002), were passaged to a new pre-heated 96-deep-well plate containing LB and a 25 % increase in antibiotic concentration in a total volume of 1 ml/well. The starting concentration was 25 % of the WT $IC_{90}$ and the WT $IC_{90}$ drug concentration was reached on the 7$^{th}$ day of the ALE (Table S3). The evolution was stopped after 18 days at a final concentration exceeding 10 fold of the WT $IC_{90}$ (Jahn et al., 2017). All antibiotic concentrations can be found in Table S3. The $IC_{90}$ of the lineages was measured on day 0, 8, 13 and 18 of the ALE in order to track the resistance evolution on the population level.

After each transfer an aliquot of 100 µl was mixed with glycerol to a final glycerol concentration of 12.5 % and stored at -80 °C. Cells were streaked on LB agar from the frozen aliquot saved on the last day with growth ($OD_{600}$ > 0.1). Some cells, were very difficult to revive as observed before (Barbosa et al. 2017). If reviving failed, cells were inoculated into liquid LB before being streaked on LB agar. If cells still failed to revive, cells were streaked from the aliquot saved the day before the last day of growth. Despite the effort, some lineages would not revive at all. A list with all lineages, their last day of growth in the ALE and the day of the ALE they have been revived from can be found in the supplementary (Table S4). One isolated colony was picked randomly for each evolved lineage, grown in LB and frozen at -80 °C for further phenotypic and genotypic characterization. Lineages adapted to the following antibiotics: Erythromycin, Sulfamethoxazole, Fosfomycin as well as the combination of Sulfamethoxazole and Trimethoprim displayed inconsistent phenotypes or did not develop resistance due to technical reasons such as drug stability after freezing. Therefore, these drugs were excluded from this study.

$IC_{90}$ determination

100 µl of LB were inoculated with pin-replicators from frozen stocks of isolated colonies and grown overnight. About $10^5$ cells were transferred with pin-replicators into plates containing a 2-fold drug gradient ranging over 10 different concentrations. Plates were grown at 37 °C for 18 h. The $OD_{600}$ was measured for each well. The $OD_{600}$ data was normalized and used to create dose-response curves in R as described before (Munck et al., 2014). In brief, percent inhibition was calculated by the following formula:

$$1 - \frac{OD_{600\ drug\ exposed} - OD_{600\ blank}}{OD_{600\ media\ exposed} - OD_{600\ blank}}$$

The $IC_{90}$ was defined as the lowest concentration of the drug that inhibited 90% of the growth (Imamovic et al., 2018; Munck et al., 2014). All $IC_{90}$ values were generated at least in two technical replicates. If the WT $IC_{90}$ differed more than 2-fold from the WT $IC_{90}$ value established before the ALE started, the $IC_{90}$ test was repeated along with the ancestor WT. No significant (Student´s t-test, $p > 0.05$) differences between the susceptibility of the WT and the media adapted WT were observed. The $IC_{90}$ values were normalized to the media adapted WT $IC_{90}$. The heatmap presenting the collateral sensitivity and resistance of the single drug evolved lineages (Fig. S2) displays the times increase of the $IC_{90}$ compared to the media adapted WT with a significance level of at least $p < 0.0001$. Significance levels were obtained as described before (Imamovic et al., 2018). Briefly, by comparing the growth data $OD_{600}$ in 10 different antibiotic concentrations of all technical and biological replicates adapted to the same drug, with all media adapted technical and biological replicates exposed to the same drug and concentration. Within the natural variation of the samples 3000 additional data points were computed to identify robust differences among samples. Times increase or decrease in growth compared to the WT was calculated in steps of 0.5 ranging from -10.5 to 10.5. Pairwise t-tests between drug adapted and media adapted data were performed and the highest times increase/the lowest times decrease with a significance value of at least $p < 0.0001$ was given as output.

Calculation of important variables

Based on the $IC_{90}$ values several calculations were made, that are explained in the following:

The evolvability index is a measure of the final phenotypic adaptation level of isolated drug-pair-evolved lineages to the individual drugs relative to isolated single-drug-evolved lineages (Munck et al., 2014). The evolvability index compares resistance evolution between drug pair and single drug evolved lineages to individual antibiotics. It was calculated as described before (Munck et al., 2014). In short, the following formula was used:

$$evolvability\ index = \frac{\frac{IC_{90}A_{AB}}{IC_{90}A_{WT}} + \frac{IC_{90}B_{AB}}{IC_{90}B_{WT}}}{\frac{IC_{90}A_{A}}{IC_{90}A_{WT}} \quad \frac{IC_{90}B_{B}}{IC_{90}B_{WT}}}}{2}$$

Two replicate lineages evolved to Amikacin and Nitrofurantion, as well as two replicate lineages evolved to Ciprofloxacin and Doxycycline had evolvability indices above 1000. They displayed extremely high $IC_{90}$ values, when tested to one of the individual drugs (Nitrofurantion/Doxycycline). As these values were way outside of a reasonable range of resistance they were treated as technical errors and therefore excluded from the entire analysis.

Drug interactions were determined for isolated colonies using a Loewe additivity model and the $IC_{90}$ as effect level. The Loewe additivity model was chosen as it assumes additive effects of identical drugs (Munck et al., 2014). This is important as drugs with the same target and drugs from the same drug class were combined in this experiment. The fractional inhibitory concentration index (FICI) was calculated according to the following formula:

$$FICI = \frac{IC_{90}AB_{WT} * \omega}{IC_{90}A_{WT}} + \frac{IC_{90}AB_{WT} * (1-\omega)}{IC_{90}B_{WT}}$$

ω is the molar fraction of A in the drug combination AB. As it was shown that additive effects are robustly detected at a cutoff between 1 and 1.25 (Meletiadis et al., 2010), we applied a low but symmetric cutoff in order to group the drug pairs into synergistic (<0.75), antagonistic (>1.5) and additive (0.75 – 1.5) combinations.

The collateral $IC_{90}$ change index was calculated for isolated colonies as described before (Munck et al., 2014). In short, the following formula was used:

$$collateral\ IC_{90}change\ index = \frac{\frac{IC_{90}A_{B}}{IC_{90}A_{WT}} + \frac{IC_{90}B_{A}}{IC_{90}B_{WT}}}{2}$$

All drug pair evolved lineages were grouped into collateral sensitivity (< 0.5), collateral resistance (>2) and neutral (0.5 – 2) effects according to the collateral $IC_{90}$ change index.

A table including all phenotypic information of the drug pair evolved lineages can be found in the supplement (Table S9).

Whole-genome sequencing and sequence analysis

1 ml LB in each well of a 96-well, deep-well plate was inoculated from frozen stocks of isolated colonies and grown at 37 °C and 600 r.p.m. overnight. Cells were spun down at 2000 r.p.m. for 3 minutes. LB was removed and replaced by DNA shielding buffer (Zymo Research). Samples were sent to BaseClear B.V. for genomic DNA extraction (ZYMO research), Nextera XT library preparation (Illumina) and 125 paired-end whole-genome Illumina HiSeq 2500 sequencing. The resulting fasta reads were used in the following workflow:

(1) Single nucleotide variants (SNPs) and small insertions and deletions (INDELS) were called using CLC Genomics workbench as described before[40]. *E. coli* reads were aligned to the *E. coli* K12 U00096 reference genome. On average, the coverage/base was at least 37 fold. For SNP calling only positions with a phred score of at least 30 at the position where the SNP occurred and at the three neighboring positions were considered. In addition, the SNP had to be detected with a frequency of at least 80 %.

(2) CLC Genomics workbench was further used to detect large insertions and deletions (large INDELS) in the reads using the INDEL function at default settings. The resulting INDELS were considered when they occurred with a frequency of more than 80 % and in more than 5 different reads.

(3) Large insertions were additionally detected by a custom made script used before[41]. The reference genomes of MG1655 as well as all open reading frames were downloaded from the NCBI nucleotide archive and used to cluster all ORFs with cd_hit (Li and Godzik, 2006). The cluster cut off was 90 % identity and coverage. Afterwards the sequenced reads from this study were quality filtered using the FASTX-Toolkit package with a minimum quality of 30 and blasted against the clustered ORFs with a word size of 16 and an e-value of 0.01. Reads, with more than 90% coverage mapping continuously to the genome, that mapped to two different clusters with an overlap between 30 and 70 % were kept for further analysis. Reads were filtered so they did not cover clusters representing adjacent genes. Finally, large insertions were only counted when they were observed in at least 5 individual reads.

(4) Gene duplications were detected using CLC workbench and a customized script in R as described before(Jahn et al., 2017). Regions > 100 bp of significantly ($p < 0.00001$) increased coverage according to a Poisson distribution were identified using CLC workbench. The identified regions were mapped to the genome and a gene that was overlapping at least 95% with a region of high coverage was counted as gene duplication.

INDELS that were detected by multiple of the parallel analyses were only counted once. Seven WT lineages adapted to the media were sequenced as a control and mutations as well as duplications found in these lineages were excluded from all lineages as they are likely mutations that have been inserted prior to the experiment or are involved in media adaptations. As no significant (Student's-test, $p > 0.05$) phenotypic difference between the resistance level of the ancestor WT and the media adapted WT lineages were identified, those genetic changes are unlikely to cause antibiotic resistance.

Jaccard´s distance

The genetic data was used to create a presence absence table for each mutations and lineage. Based on this matrix the Jaccard´s distance was calculated using the jaccardSets function in R from the package bayesbio(McKenzie, 2016).

Analysis of similarity

Based on the genetic data including SNPs, INDELS and gene duplications, a binary presence absence data matrix was created for each lineage and all genes. The matrix was summed for all replicates of the same condition and subsequently used to calculate a dissimilarity matrix with the package "vegan" in R using Euclidian distance (Oksanen et al., 2019). We performed an analysis of similarities with the anosim function from the package "vegan" in R for the entire dataset in order to test whether significant differences between groups could be expected (Oksanen et al., 2019). Our dataset included significant ($p < 0.01$) differences between lineages adapted to different drugs, wherefore we calculated pair-wise differences between different drug-adapted groups of replicates with the same methodology and 1000 permutations. We calculated three different similarities for each drug pair: first, we compared lineages evolved to both single drugs constituting the pair, second, we compared the group of one of the single drug adapted lineages to the drug pair evolved lineages and third, we compared the other single drug evolved lineages to the drug pair evolved ones. Groups were considered to be significantly different when they had a $p$-value smaller than 0.005 and

an R statistics greater than 0.2. A R statistics of 0.2 has previously been described as measure for mild similarities between groups (Oksanen et al., 2019). The results were aggregated with the package "data.table" (Dowle and Srinivasan, 2018).

Data availability and code

Genomic data is available in NCBI under the accession number SUB5823083. All phenotypic data and scripts can be provided upon request. For the calculations and different analysis the following R packages have been utilized: "plyr" (Wickham, 2011), "dplyr" (Wickham et al., 2018), "tidyr" (Wickham and Henry, 2018), "ggplot2" (Wickham, 2016), "data.table" (Dowle and Srinivasan, 2018), "gdata" (Warnes et al., 2017), "SciViews" (Grosjean, 2018), "drc" (Ritz et al., 2015), "scales" (Wickham, 2018), "gridExtra" (Auguie,, 2017), "cowplot" (Wilke, 2018), "stringr" (Wickham, 2018), "ggpubr" (Kassambara, 2018), "magrittr" (Bache and Wickham, 2014). For Fig. 1 RawGraphs (Mauri et al., 2017) was used to create the figure. All figures were edited in Abode Illustrator.

**References**

**Auguie, B.** (2017). gridExtra: Miscellaneous Functions for "Grid" Graphics. R package version 2.3. https://CRAN.R-project.org/package=gridExtra

**Bache, S.M., and Wickham, H.** (2014). magrittr: A Forward-Pipe Operator for R. R package version 1.5. https://CRAN.Rproject.org/package=magrittr

**Bantar, C.** *et al.* Replacement of Broad-Spectrum Cephalosporins by Piperacillin-Tazobactam: Impact on Sustained High Rates of Bacterial Resistance. *Antimicrob. Agents Chemother.* 48, 392–395 (2004).

**Bailey, S.F., Rodrigue, N., and Kassen, R.** (2015). The Effect of Selection Environment on the Probability of Parallel Evolution. *Mol. Biol. Evol. 32*, 1436–1448.

**Barbosa, C., Beardmore, R., Schulenburg, H., and Jansen, G.** (2018). Antibiotic combination efficacy (ACE) networks for a Pseudomonas aeruginosa model. *PLoS Biol. 16*.

**Barbosa, C., Trebosc, V., Kemmer, C., Rosenstiel, P., Beardmore, R., Schulenburg, H., and Jansen, G.** (2017). Alternative Evolutionary Paths to Bacterial Antibiotic Resistance Cause Distinct Collateral Effects. *Mol. Biol. Evol. 34(9):*2229-2244

**Baym, M., Stone, L.K., and Kishony, R**. (2016). Multidrug evolutionary strategies to reverse antibiotic resistance. *Science 351*, aad3292.

**Beutner, E.H., Doyle, W.M., and Evander, L.C.** (1963). Collateral Susceptibility of Isoniazid-Resistant Tubercle Bacilli To Nitrofurans. *Am. Rev. Respir. Dis. 88*, 712–715.

**Bliziotis, I.A., Samonis, G., Vardakas, K.Z., Chrysanthopoulou, S., and Falagas, M.E**. (2005). Effect of Aminoglycoside and β-Lactam Combination Therapy versus β-Lactam Monotherapy on the Emergence of Antimicrobial Resistance: A Meta-analysis of Randomized, Controlled Trials. *Clin. Infect. Dis. 41*, 149–158.

**Blomberg, B., Spinaci, S., Fourie, B., and Laing, R.** (2001). The rationale for recommending fixed-dose combination tablets for treatment of tuberculosis. Bull. *World Health Organ*. *79*, 61–68.

**Bodilsen, J., Brouwer, M.C., Kjærgaard, N., Sirks, M.J., van der Ende, A., Nielsen, H., and van de Beek, D.** (2018). Community-acquired meningitis in adults caused by Escherichia coli in Denmark and The Netherlands. *J. Infect. 77*, 25–29.

**Brook, I.** (1989). Inoculum effect. *Rev. Infect. Dis. 11*, 361–368.

**Bueno, M.L., Dexter, K.G., Pennington, R.T., Pontara, V., Neves, D.M., Ratter, J.A., and Oliveira-Filho, A.T. de** (2018). The environmental triangle of the Cerrado Domain: Ecological factors driving shifts in tree species composition between forests and savannas. *J. Ecol. 106*, 2109–2120.

**Chevereau, G., and Bollenbach, T.** (2015). Systematic discovery of drug interaction mechanisms. *Mol. Syst. Biol. 11*.

**Dowle, M. and Srinivasan, A.** (2018). data.table: Extension of `data.frame`. R package version 1.11.8. https://CRAN.R-project.org/package=data.table

**de Evgrafov, M.R., Gumpert, H., Munck, C., Thomsen, T.T., and Sommer, M.O.A.** (2015). Collateral resistance and sensitivity modulate evolution of high-level resistance to drug combination treatment in Staphylococcus aureus. *Mol. Biol. Evol. 32(5):*1175-1185

**Gonzales, P.R., Pesesky, M.W., Bouley, R., Ballard, A., Biddy, B.A., Suckow, M.A., Wolter, W.R., Schroeder, V.A., Burnham, C.-A.D., Mobashery, S., et al.** (2015). Synergistic, collaterally sensitive β-lactam combinations suppress resistance in MRSA. *Nat. Chem. Biol. 11*, 855–861.

**Grosjean, Ph.** (2018). SciViews-R. UMONS, Mons, Belgium. URL http://www.sciviews.org/SciViews-R.

**Hegreness, M., Shoresh, N., Damian, D., Hartl, D., and Kishony, R**. (2008). Accelerated evolution of resistance in multidrug environments. *Proc. Natl. Acad. Sci. 105*, 13977–13981.

**Imamovic, L., and Sommer, M.O.A.** (2013). Use of Collateral Sensitivity Networks to Design Drug Cycling Protocols That Avoid Resistance Development. *Sci. Transl. Med. 5*, 204ra132-204ra132.

**Imamovic, L., Ellabaan, M.M.H., Dantas Machado, A.M., Citterio, L., Wulff, T., Molin, S., Krogh Johansen, H., and Sommer, M.O.A.** (2018). Drug-Driven Phenotypic Convergence Supports Rational Treatment Strategies of Chronic Infections. *Cell 172*, 121-134.e14.

**Jahn, L.J., Munck, C., Ellabaan, M.M.H., and Sommer, M.O.A.** (2017). Adaptive Laboratory Evolution of Antibiotic Resistance Using Different Selection Regimes Lead to Similar Phenotypes and Genotypes. *Front. Microbiol. 8*.

**Jahn, L.J., Porse, A., Munck, C., Simon, D., Volkova, S., and Sommer, M.O.A.** (2018). Chromosomal barcoding as a tool for multiplexed phenotypic characterization of laboratory evolved lineages. *Sci. Rep. 8*, 6961.

**Jansen, G., Barbosa, C., and Schulenburg, H.** (2013). Experimental evolution as an efficient tool to dissect adaptive paths to antibiotic resistance. *Drug Resist. Updat. 16*, 96–107.

**Jolivet-Gougeon, A., Kovacs, B., Le Gall-David, S., Le Bars, H., Bousarghin, L., Bonnaure-Mallet, M., Lobel, B., Guille, F., Soussy, C.-J., and Tenke, P.** (2011). Bacterial hypermutation: clinical implications. *J. Med. Microbiol. 60*, 563–573.

**Kassambara, A.** (2018). ggpubr: 'ggplot2' Based Publication Ready Plots. R packageversion 0.2. https://CRAN.R-project.org/package=ggpubr

**Laehnemann, D., Peña-Miller, R., Rosenstiel, P., Beardmore, R., Jansen, G., and Schulenburg, H.** (2014). Genomics of Rapid Adaptation to Antibiotics: Convergent Evolution and Scalable Sequence Amplification. *Genome Biol. Evol*. *6*, 1287–1301.

**Lazar, V., Pal Singh, G., Spohn, R., Nagy, I., Horvath, B., Hrtyan, M., Busa-Fekete, R., Bogos, B., Mehi, O., Csorgo, B., et al.** (2014). Bacterial evolution of antibiotic hypersensitivity. *Mol. Syst. Biol. 9*, 700–700.

**Lee, H.H., Molla, M.N., Cantor, C.R., and Collins, J.J.** (2010). Bacterial charity work leads to population-wide resistance. *Nature 467*, 82–85.

**Leibovici, L., Paul, M., Poznanski, O., Drucker, M., Samra, Z., Konigsberger, H., and Pitlik, S.D.** (1997). Monotherapy versus beta-lactam-aminoglycoside combination treatment for gram-negative bacteremia: a prospective, observational study. *Antimicrob. Agents Chemother. 41*, 1127–1133.

**Levin-Reisman, I., Ronin, I., Gefen, O., Braniss, I., Shoresh, N., and Balaban, N.Q.** (2017). Antibiotic tolerance facilitates the evolution of resistance. *Science 355*, 826–830.

**Li, W., and Godzik, A.** (2006). Cd-hit: a fast program for clustering and comparing large sets of protein or nucleotide sequences. *Bioinformatics 22*, 1658–1659.

**Lipcsey, M., Castegren, M., Furebring, M., Sjölin, J.** (2018). Should the Aminoglycoside β-Lactam Combination Be Abandoned in All Severely Ill Patients With Presumed Gram-Negative Infection? | *Clinical Infectious Diseases* | *Oxford Academic*.1537-6591

**Lipsitch, M., and Levin, B.R.** (1997). The population dynamics of antimicrobial chemotherapy. *Antimicrob. Agents Chemother*. *41*, 363–373.

**Luepke, K.H., Suda, K.J., Boucher, H., Russo, R.L., Bonney, M.W., Hunt, T.D., and Mohr, J.F.** (2017). Past, Present, and Future of Antibacterial Economics: Increasing Bacterial Resistance, Limited Antibiotic Pipeline, and Societal Implications. *Pharmacother. J. Hum. Pharmacol. Drug Ther. 37*, 71–84.

**MacPherson, A., and Nuismer, S.L.** (2017). The probability of parallel genetic evolution from standing genetic variation. *J. Evol. Biol*. *30*, 326–337.

**Mauri, M., Elli, T., Caviglia, G., Uboldi, G., & Azzi, M***.* (2017). RAWGraphs: A Visualisation Platform to Create Open Outputs. In *Proceedings of the 12th*

*Biannual Conference on Italian SIGCHI Chapter* (p. 28:1–28:5). New York, NY, USA: ACM. https://doi.org/10.1145/3125571.3125585

**McKenzie, A.** (2016). bayesbio: Miscellaneous Functions for Bioinformatics and Bayesian Statistics.

**Meletiadis, J., Pournaras, S., Roilides, E., and Walsh, T.J.** (2010). Defining Fractional Inhibitory Concentration Index Cutoffs for Additive Interactions Based on Self-Drug Additive Combinations, Monte Carlo Simulation Analysis, and In Vitro-In Vivo Correlation Data for Antifungal Drug Combinations against Aspergillus fumigatus. *Antimicrob. Agents Chemother*. *54*, 602–609.

**Minato, Y., Dawadi, S., Kordus, S.L., Sivanandam, A., Aldrich, C.C., and Baughn, A.D.** (2018). Mutual potentiation drives synergy between trimethoprim and sulfamethoxazole. *Nat. Commun. 9*, 1003.

**Munck, C., Gumpert, H.K., Wallin, A.I.N., Wang, H.H., and Sommer, M.O.A.** (2014). Prediction of resistance development against drug combinations by collateral responses to component drugs. *Sci. Transl. Med. 6*, 262ra156-262ra156.

**Oksanen, J., Blanchet, F.G., Friendly, M., Kindt, R., Legendre, P., McGlinn, D., Minchin, P.R., O'Hara, R. B., Simpson, G.L., Solymos, P., Henry, M., Stevens, H., Szoecs, E. and Wagner, H.** (2019). vegan: Community Ecology Package. R package version 2.5-5. https://CRAN.R-project.org/package=vegan

**Okusu, H., Ma, D., and Nikaido, H.** (1996). AcrAB efflux pump plays a major role in the antibiotic resistance phenotype of Escherichia coli multiple-antibiotic-resistance (Mar) mutants. *J. Bacteriol. 178*, 306–308.

**Paul, M., Lador, A., Grozinsky-Glasberg, S., Leibovici, L.** (2014). Beta lactam antibiotic monotherapy versus beta lactam-aminoglycoside antibiotic combination therapy for sepsis. *Cochrane Library*. 1465-1858

**Ritz, C., Baty, F., Streibig, J. C., Gerhard, D.** (2015) Dose-Response Analysis Using R *PLOS ONE*, 10(12), e0146021

**Pena-Miller, R., Laehnemann, D., Jansen, G., Fuentes-Hernandez, A., Rosenstiel, P., Schulenburg, H., and Beardmore, R.** (2013). When the Most Potent Combination of Antibiotics Selects for the Greatest Bacterial Load: The Smile-Frown Transition. *PLoS Biol 11*, e1001540.

**Skorup, P., Maudsdotter, L., Lipcsey, M., Castegren, M., Larsson, A., Jonsson, A.-B., and Sjölin, J.** (2014). Beneficial Antimicrobial Effect of the Addition of an Aminoglycoside to a β-Lactam Antibiotic in an E. coli Porcine Intensive Care Severe Sepsis Model. *PLOS ONE 9*, e90441.

**Stokes, J.M., MacNair, C.R., Ilyas, B., French, S., Côté, J.-P., Bouwman, C., Farha, M.A., Sieron, A.O., Whitfield, C., Coombes, B.K., et al.** (2017).

Pentamidine sensitizes Gram-negative pathogens to antibiotics and overcomes acquired colistin resistance. *Nat. Microbiol. 2*, 17028.

**Suzuki, S., Horinouchi, T., and Furusawa, C**. (2015). Suppression of antibiotic resistance acquisition by combined use of antibiotics. *J. Biosci. Bioeng. 120*, 467–469.

**Szybalski, W., and Bryson, V.** (1952). Genetic studies on microbial cross resistance to toxic agents I.: Cross Resistance of Escherichia coli to Fifteen Antibiotics1, 2. *J. Bacteriol. 64*, 489.

**Tepekule, B., Uecker, H., Derungs, I., Frenoy, A., and Bonhoeffer, S.** (2017). Modeling antibiotic treatment in hospitals: A systematic approach shows benefits of combination therapy over cycling, mixing, and mono-drug therapies. *PLOS Comput. Biol*. *13*, e1005745.

**Torella, J.P., Chait, R., and Kishony, R.** (2010). Optimal Drug Synergy in Antimicrobial Treatments. *PLoS Comput. Biol. 6*.

**Tyers, M., and Wright, G.D.** (2019). Drug combinations: a strategy to extend the life of antibiotics in the 21st century. *Nat. Rev. Microbiol. 17*, 141–155.

**Ventola, C.L.** (2015). The Antibiotic Resistance Crisis. *Pharm. Ther. 40*, 277–283.

**Wahl, L.M., Gerrish, P.J., and Saika-Voivod, I.** (2002). Evaluating the Impact of Population Bottlenecks in Experimental Evolution. *Genetics 162*, 961–971.

**Warnes, G.R., Bolker, B., Gorjanc, G., Grothendieck, G., Korosec, A., Lumley, T., MacQueen, D., Magnusson, A., Rogers, J., and others** (2017). gdata: Various R Programming Tools for Data Manipulation. R package version 2.18.0. https://CRAN.R-project.org/package=gdata

**Wickham, H.** (2011). The Split-Apply-Combine Strategy for Data Analysis. Journal of Statistical Software, 40(1), 1-29. URL http://www.jstatsoft.org/v40/i01/

**Wickham, H.** (2016). ggplot2: Elegant Graphics for Data Analysis. *Springer-Verlag New York*, 2016.

**Wickham, H.** (2018). stringr: Simple, Consistent Wrappers for Common String Operations. R package version 1.3.1. https://CRAN.R-project.org/package=stringr

**Wickham, H.** (2018). scales: Scale Functions for Visualization. R package version 1.0.0. https://CRAN.R-project.org/package=scales

**Wickham, H. and Henry, L.** (2018). tidyr: Easily Tidy Data with 'spread()' and 'gather()'Functions. R package version 0.8.2. https://CRAN.R-project.org/package=tidyr

**Wickham, H., François, R., Henry L. and Müller, K.** (2018). dplyr: A Grammar of DataManipulation. R package version 0.7.7. https://CRAN.R-project.org/package=dplyr

**Wilke, C.O.** (2018). cowplot: Streamlined Plot Theme and Plot Annotations for 'ggplot2'. R package version 0.9.3. https://CRAN.R-project.org/package=cowplot

**Wong, A.** (2017). Epistasis and the Evolution of Antimicrobial Resistance. *Front. Microbiol. 8*.

**Woodford, N., and Ellington, M.J.** (2007). The emergence of antibiotic resistance by mutation. *Clin. Microbiol. Infect. 13*, 5–18.

**World Health Organization**, and Global Tuberculosis Programme (2016). WHO treatment guidelines for drug-resistant tuberculosis: 2016 update.

**Yu, E.W., Aires, J.R., and Nikaido, H.** (2003). AcrB Multidrug Efflux Pump of Escherichia coli: Composite Substrate-Binding Cavity of Exceptional Flexibility Generates Its Extremely Wide Substrate Specificity. *J. Bacteriol. 185*, 5657–5664.

**Acknowledgements**

C. Munck and L. Imamovice advised on the panel of individual drugs to use and on the adaptive evolution experiment protocol. O. Bitterlin assisted C. Bradshaw in programming the robot used for preparing plates for the evolution experiment and for $IC_{90}$ determination. In addition, we thank J.J. Collins, A. Porse, D. Kell, J. Yang, A. Lopatkin, S. Li, M.A. Misiakou and A.S. Hauser for helpful discussions and input on data representation.

**Funding**

This work was supported by the European Union's Horizon 2020 research and innovation program under the Marie Sklodowska-Curie grant agreement No 642738, MetaRNA as well from the European Union's Horizon 2020 (ERC-2014-StG) under grant agreement 638902, LimitMDR. In addition, funding was received from Danish Council for Independent Research, Sapere Aude Program DFF 4004-00213 and from The Novo Nordisk Foundation under NFF grant number: NNF10CC1016517.

**Author contribution**

MOAS and LJJ conceived the project. CB, LJJ and DS prepared plates used for the adaptive laboratory evolution experiment with help of a Hamilton robot. LJJ, DS and MJ conducted all experimental work. LJJ analyzed and visualized the data. MMHE analyzed the genomic data for large insertions and deletions. LJJ wrote the manuscript with input from MOAS.

**Author affiliation**

Novo Nordisk Foundation Center for Biosustainability, Technical University of Denmark, Lyngby, Denmark.